SQU Journal for Science, 2015, 20(1), 39-54
© 2015 Sultan Qaboos University

Mobilization and Redistribution of Elements in Laterites of Semail Ophiolite, Oman: A Mass Balance Study

Salah Al Khirbash* and Khadija Semhi

*Department of Earth Sciences, College of Science, Sultan Qaboos University, P.O. Box: 36, PC 123, Al-Khod, Muscat, Sultanate of Oman. *Email: khirbash @squ.edu.om.*

ABSTRACT: Several samples of laterites were collected from four paleosol profiles, Ibra, East Ibra, Al-Russayl, and Tiwi representing the vertical lithological variation within each profile. The mineralogical and geochemical composition of laterites in every section revealed differences in thickness and redistribution of elements reflecting different conditions of weathering processes. Elemental mass balance was calculated for every profile relative to the parent rock. The results indicated redistribution of elements from the surface to deeper zones with an enrichment of elements in the saprolite and oxide zones. Among the different sections, the profile of East Ibra composite 1 and 2 is characterized by high concentration of all elements compared to the other profiles. Sc/Fe ratio in different zones indicates low values for the profile of Tiwi profile 1, Ibra profile and Al-Russayl composite 2 and 3 profile due to the significant enrichment of Fe in these zones independently of redox conditions. Large fluctuations characterize Th/U ratios and reflect redox condition more reduced in Tiwi area than in East Ibra and Al-Russayl areas.

Keywords: Laterite; Oman; Mass balance; Profile; Enrichment; Economy.

حركة وإعادة توزيع العناصر في تربة اللاتريت لصخور اوفيوليت سمائل، سلطنة عمان: دراسة التوازن الكتلي

صلاح ع. الخرباش و خديجة سمحي

ملخص: تتمحور الدراسة الحالية حول تربة اللاتريت حيث تم جمع عدة عينات من عدة مقاطع لتربة اللاترايت لتمثل الطبقات الأفقية للتربة. شملت هذه الدراسة مناطق إبرا وشرق إبرا والرسيل و طيوي. بينت نتائج دراسة المكونات المعدنية والخصائص الجيوكميائية لكل مقطع تفاوتا بين مختلف الطبقات خاصة في سمكها وإعادة توزيع وتركيز مختلف العناصر مما يكون راجعا الى اختلافات في عوامل التجوية من منطقة إلى أخرى. بناء على نتائج حساب التوازن الكتلي لكل طبقة مقارنة مع تركيب الصخرة الأساسية للتربة تبين أن هناك إما تراكم أو ترشح للعناصر عبر مقطع التربة من السطح ألى أسفل التربة نتيجة لعمليات التجوية. أن نسبة العناصر تزايدت في كل من طبقة السابرولايت و طبقة الاكساييد وخاصة في مقطع شرق إبرا حيث تميزت بتراكيز عالية لمعظم العناصر. وعند دراسة نسبة عنصر السكانديوم على الحديد في التربة من مختلف مناطق هذه الدراسة(طيوي و إبرا والرسيل) اتضح لنا قيم ضعيفة لهذه النسبة مما يعزى ذلك لتراكم مهم للحديد اثناء عمليات التجوية. كما بينت النسبة بين عنصري الثوريوم واليورانيوم بأن عوامل التجوية بمنطقة طوي كانت أقل مأكسدة مما هو عليه في شرق إبرا و الرسيل.

كلمات مفتاحية: لاترايت، تربة، تراكم، حساب توازن الكتلي وعمان.

1. Introduction

Lateritic weathering is an important surficial erosional process which is active in the superficial zone of tropical regions. All laterites are marked by an enrichment of iron and a decrease of silica together with the highly soluble alkalis and alkaline earths as well as rare earth elements [1]. The composition and properties of laterites are controlled by the chemical and physical features of the parent rock.

Mobilization of trace elements during lateritization has been investigated in several studies [2-6]. This mobilization is dependent on the type of parent rock and the weathering conditions (T, Eh, and solutions). Lateritization of ultramafic rocks such as peridotite results in an enrichment of Ni. Most of the world's laterites are found in tropical areas such as Indonesia, the Philippines and New Caledonia but some are also found in Australia, Brazil and West Africa [7-11].

In this study, a mass balance was calculated in laterites in Oman in order to determine the redistribution and mobilization of trace elements in the different lateritic zones developed on mafic and ultramafic rocks in this arid area during the Cretaceous time.

The current research is part of an ongoing research project by the first author, investigating lateritic soils from the Northern Oman Mountains, where the samples were collected from each zone (from the surface downward to the parent rock) of the investigated laterite profiles [12]. The parent rocks consist either of layered gabbro or peridotite of about c.96.4 Ma [13].

2. Geological background

The development of lateritic paleosol profiles in Oman is mainly related to the late Cretaceous (Coniacian to late Campanian) tectonic evolution of the Oman Mountains, which are part of the Alpine-Himalayan fold belt [14,15]. A detailed description of these laterites is given in [12, 16, 17]. The laterites of the Oman Mountains belong to the Qahlah Formation that lies unconformably on the obducted Semail ophiolite (96.4 Ma.) [13,18] and grades into the Late Campanian–Maastrichtian Simsima Formation. The Qahlah Formation represents the most basal, post-obduction terrigenous clastic facies in Oman [14] and mainly contains conglomerate, sandstone, and siltstone [19]. This formation was assigned a Maastrichtian age [14] based on the presence of *Loftusia*. The Late Cretaceous laterites generally occur as patches having a lateral extension of more than 100 km, but are entirely absent at some locations [12].

The mineralogical and geochemical charcterization of nine laterite profiles from four separate areas (Ibra, East Ibra, Al-Russayl, and Tiwi) located along a NW-SE transect across the Oman Mountains (Figure 1) have been previously reported [1,12,16,17], where they showed variations in their thickness as well as in their geochemical and mineralogical characteristics. For the purpose of this study, these nine profiles have been combined into seven profiles (Figure 2), where the East Ibra profiles # 1 and 2 were combined as one profile (designated as composite profile #1 and #2) and Al-Russayl profiles # 2 and 3 were combined as one profile (designated as composite profile #1 and #2).

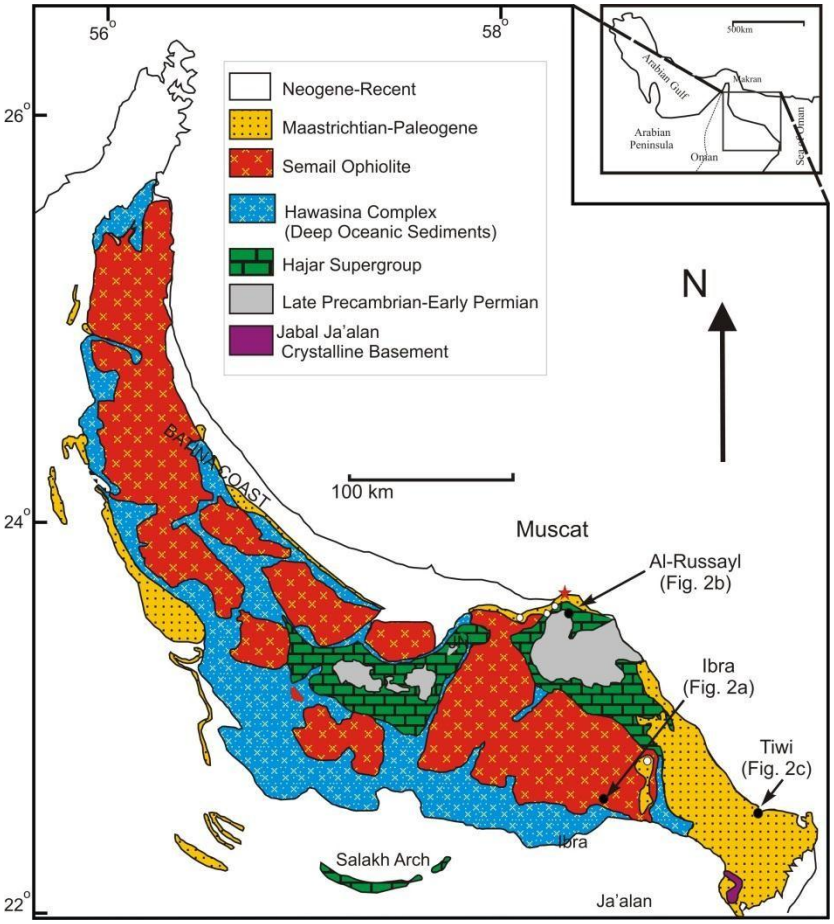

Figure 1. Geological and location map of the studied areas (adapted from [12,19]).

The following lateritic zones were identified from the base upward: a) a protolith; b) a saprolite laterite; c) an oxide laterite (locally pisolitic and with multiple silcrete layers); and d) a clay laterite (Figure 2) [16].

a. Protolith corresponds either to serpentinized peridotite (East of Ibra, Al-Russayl and Tiwi profiles) or to layered gabbro (Ibra profile) of the Late Cretaceous Semail ophiolite. The serpentinized peridotite is > 20 m thick and occurs as a fine-grained, black to green rock. The layered gabbro protolith is > 20 m thick and consists of a coarse-grained dark green rock.

b. Saprolite (3-60 m thick) is characterized by a pale reddish-brown to greenish color and abundant blocks ranging in size from a few cms to >6 m. The lower parts of the saprolite zone usually consist of greenish-white, friable material, while the upper parts consist of harder, reddish-brown material with abundant ferruginous pellets (pisoliths).
c. Oxide zone (1.5 to 84 m thick) is characterized by massive to nodular facies of yellowish, goethite-rich limonite, as well as massive hematite. It includes several 0.5 to 1 m thick, white to grey color, silcrete layers.
d. Clay laterite (1.5 to 15 m thick) is made up of hard, dark-brown material in the lower parts and light-brown, soft and friable fine-grained material in the upper parts.

These paleosol lateritic profiles are capped unconformably either by clastics of the Upper Cretaceous Qahlah Formation, which is the case at East Ibra, or by Palaeogene carbonates of the Jafnayn or Abat Formations at Ibra, Tiwi and Al-Russayl areas [16].

3. Materials and methods

Several samples were collected vertically throughout the different profiles to represent the various lateritic zones (Figure 2). All samples were dried overnight at about 60 ºC. After drying, they were crushed and sieved to a fraction less than 2 mm and homogenized in an agate mill. Two batches of each sample were prepared. One batch was used for identification of mineral composition while the other was used for chemical analyses. For chemical analysis, a 0.5 g sample was digested in aqua regia at 95 ºC in a microprocessor controlled hot block for 2 hours. The solution was diluted and analyzed for trace elements by ICP/MS using a Perkin Elmer SCIEX ELAN 9000 [12].

International certified reference materials USGS GXR-1, GXR-2, GXR-4 and GXR-6 were analyzed at the beginning and at the end of each batch of samples. Internal control standards were analyzed every 10 samples and a duplicate was run for every 10 samples. The detection limit varied between 0.01 and 0.5 ppb. Chemical composition was determined by (ICP-AES) for major elements. Analytical precisions ranged between 5 and 10%. All geochemical analyses were carried out at the Activation Laboratories Ltd (Canada).

The qualitative mineralogical analysis was carried out in the Department of Earth Sciences of Sultan Qaboos University (Oman) using X'Pert PRO X-ray diffraction with a 45 mA, 40 kV generator settings.

4. Results

a. Mineralogy of the laterite zones: Mineralogy of laterites in the Oman Mountains is discussed in detail by Al-Khirbash *et al*. [16]. The following paragraphs summarize the most important lithological and mineralogical composition of the various zones of the investigated laterite sections.
i. Protolith: The protolith is composed of either black to green peridotite rock (the East Ibra and Tiwi profiles) or of dark green coarse-grained layered gabbro (Ibra profile). XRD analyses showed the presence of lizardite, kaolinite, maghemaite, antigorite, and clinochrysotile, in addition to some other Ni bearing minerals (Figure 2).
ii. Saprolite laterite: The initial texture of the protolith is fully preserved in this zone and composed mainly of lizardite (after pyroxenes), some altered plagioclase, amorphous iron oxides, and quartz. The mineral composition obtained through XRD analyses is given in Figure 2.
iii. Oxide laterite: Hematite and goethite are the primary components of this zone giving a reddish colored appearance to the rock. The results of the XRD mineral analyses are given in Figure 2.
iv. Clay laterite: This zone is characterized by fine-grained, compact iron-stained-looking material. Kaolinite and iron oxides are the main components. Calcite and quartz-filling fractures and blebs of amorphous silica are also observed. XRD mineral analyses are given in Figure 2.
v. Silcrete layers: Several silcrete layers are observed at different levels within the oxide zone, particularly in the profiles of East Ibra and Al-Russayl (Figure 2). These silcrete layers are hard, displaying massive vesicular and concretionary textures, and are composed of fine-grained amorphous silica or quartz. X-Ray diffraction analysis confirmed the presence of quartz, hematite, and calcite in the silcrete layers.
vi. Ferricrete layers: The ferricrete layers have complex fabrics and are mainly composed of hematite and goethite (Al-Russayl profile #1) or of magnetite and hematite (Ibra profile) (Figure 2).

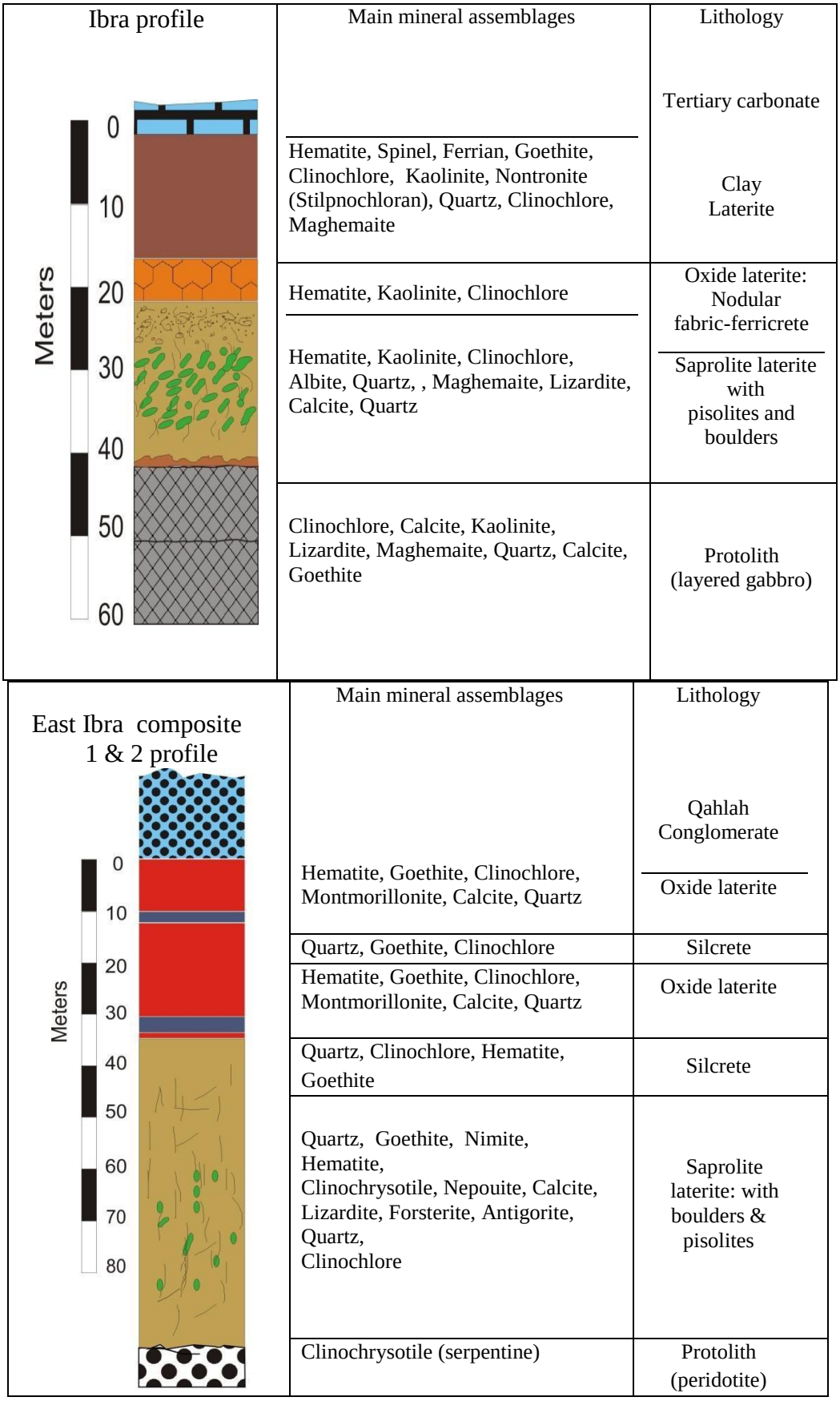

Figure 2. Lithostratigraphic description and XRD data of the studied laterite profiles.

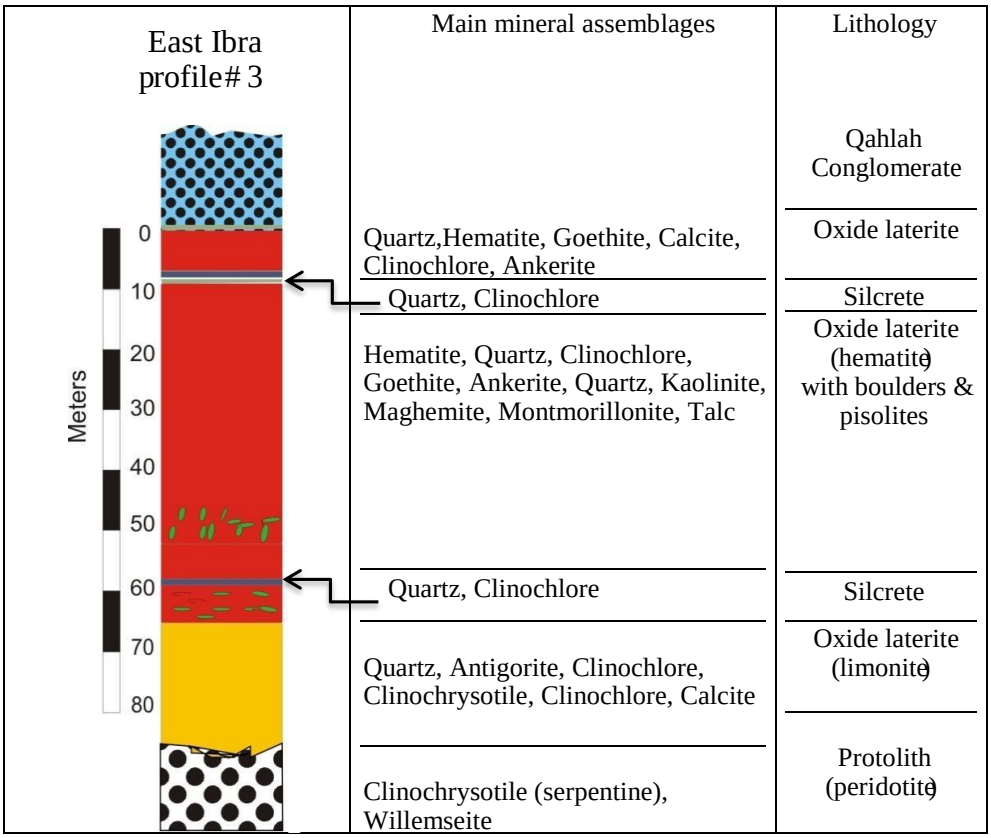

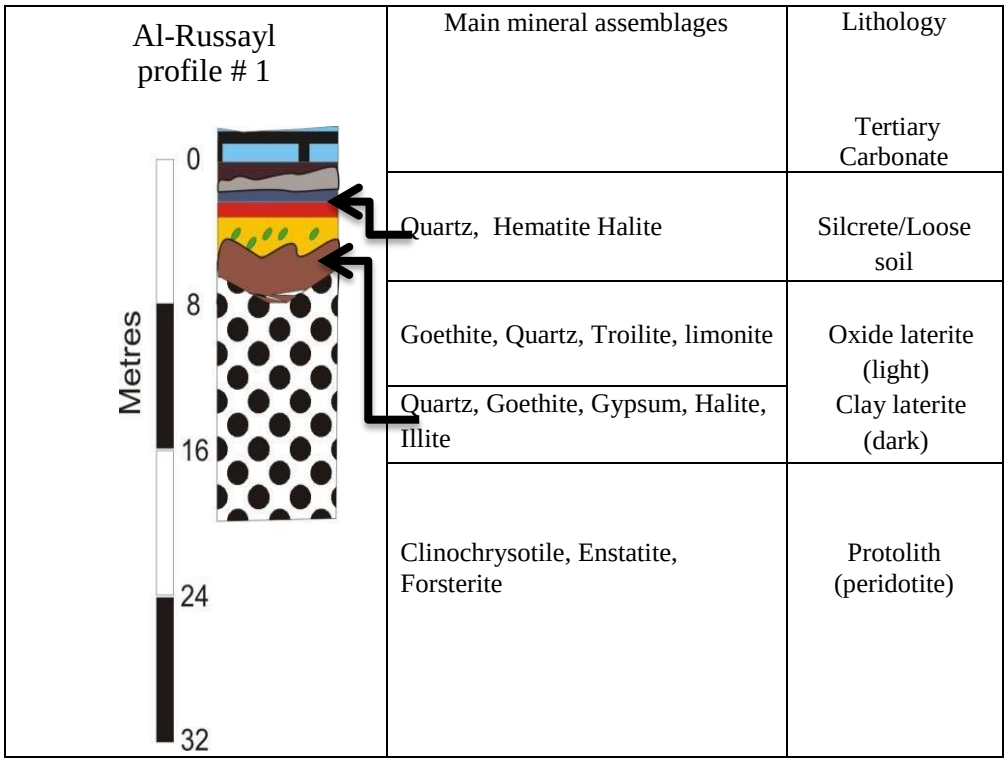

Figure 2. Continued

Al- Russayl composite 2 & 3 profile	Main mineral assemblages	Lithology
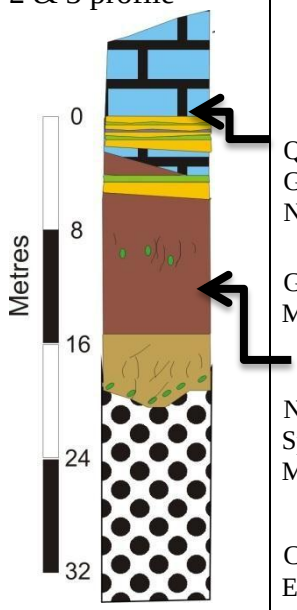	Quartz, Calcite, Lizardite, Saponite, Goethite, Montmorillonite Nontronite, Allanite, Illite Goethite Lizardite, Quartz, Montmorillonite (bentonite) Nontronite, Lizardite,Ringwoodite, Spinel, Quartz, Clinochlore, Montmorillonite Clinochrysotile, Forsterite, Enstatite,Augite	Tertiary Carbonate Oxide laterite (light) Clay laterite (dark) Saprolite Laterite: with boulders Protolith (peridotite)

Tiwi profile # 1	Main mineral assemblages	Lithology
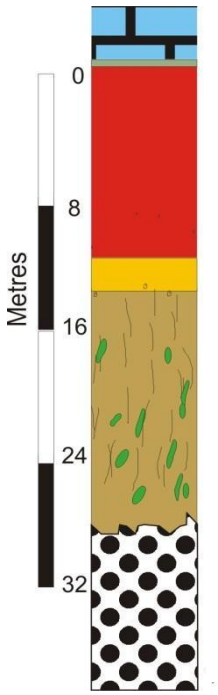		Tertiary Carbonate
	Hematite, Spinel, Bohmite, Kaolinite, Dolomite,Goethite, Clinoclore, Illite	Oxide laterite (hematite with limonite at base)
	Dolomite, Lizardite, Calcite, Talc Hematite	Saprolite laterite: with boulders & pisolites
	Lizardite, Dolomite	Protolith (peridotite)

Figure 2. Continued

Tiwi profile # 2 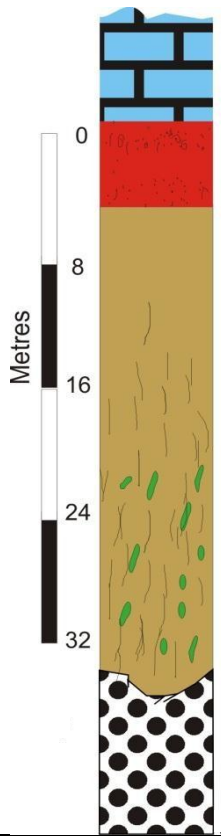	Main mineral assemblages	Lithology Tertiary Carbonate
	Hematite, Goethite, Clinochlore, Willemseite	Oxide laterite
	Clinochrysotile (serpentine), Dolomite, Lizardite, Forsterite, Actinolite, Ankerite	Saprolite laterite: with boulders & pisolites
	Lizardite, Dolomite, Augite	Protolith (peridotite)

Figure 2. continued

b. Geochemistry

The geochemical characteristics of different sections in the same profile are given in detail in [12]. In this paper, geochemical composition of the laterite will be briefly described. Average concentrations of elements at different zones are given in Table 1.

i. Ibra profile: Geochemical investigation of trace elements in Ibra profile revealed that the content of Ni is higher in the serpentinized peridotite than in the other zones (Table 1). The Ni average content increases from 2000 ppm in the protolith zone to 3000, 5000, 8000, 9000 and 18000 ppm in the saprolite, oxide, clay laterites, Fe bed/ferricrete and serpentinized peridotite, respectively. The highest concentrations of Cr were observed in the clay zone while the highest concentrations of Zn were observed in the ferricrete zone (see Table 1). The concentrations of most of the elements in the clay zone remain lower than in the other zones except for Pb and Ba.

ii. East Ibra profiles: In East Ibra profile, concentrations of trace elements exhibit significant fluctuations from the surface to the zone at 50 m depth. The Ni contents, for example, in the East Ibra composite 1 and 2 profile range from 1000 to 9000 with important enrichment in the oxide zone (Table 1). Further, high concentrations of Cr, V, Zn, Sr and Ba were also observed in the oxide zone (Table 1). In East Ibra 3 profile, the highest concentrations of elements were observed in the oxide zone, except for Sr, Ba and possibly Pb, which have leached to the lower zones (clay zone). The silcrete layer remains less enriched in most elements, when compared with the protolith zone.

iii. Al-Russayl profile: The lateral distribution of trace elements through the Al-Russayl profile #1, shows that the concentrations of Ni, V, Cr and Zn are higher in the oxide zone than in the other zones (see Table 1) while Ba, Sr and Pb have accumulated more in the ferricrete zone. In Al-Russayl composite profile 2 and 3, most of the elements, except Ba and Pb, are enriched in the clay zone when compared to the other investigated zones.

iv. Tiwi profile: The lateral distribution of trace elements through the Tiwi profile #1 showed that all elements (except Ni) are more concentrated in the clay zone, compared to the saprolite and oxide zones. The distribution of elements in Tiwi profile #2 shows that their concentrations in the oxide zone are higher than in the saprolite zone (see Table 1).

Table 1. Geochemical analyses (in ppm) of the studied laterites, Oman Mountains.

Profile	Zone/ Element	Fe	Mn	Ti	Cr	Ni	Co	V	Zn	Rb	Sr	Zr	Ba	La	Pb	Sc
Ibra	protolith	58496	859	120	2737	2000	100	2.3	25.0	0.4	23.4	0.1	14.8	1.2	0.2	7.7
	Serpentinite/ peridotite	72846	4101	300	2737	18000	1000	32.5	71.2	0.4	189.5	0.1	22.3	8.8	0.3	17.8
	saprolite	250204	1505	4796	6158	3000	100	129.8	20.1	0.2	108.7	3.3	14.2	3.0	1.9	32.2
	oxide	440897	729	1799	30105	5000	100	101.3	25.3	< 0.1	37.6	2.2	8.2	1.7	4.8	47.2
	clay	325631	1232	1799	43789	8000	1000	79.3	21.0	2.3	68.1	0.8	17.0	7.0	12.2	42.8
	ferricrete	396752	2528	1799	30105	9000	1000	126.5	115.9	< 0.1	152.0	1.9	12.5	13.9	7.1	60.3
East Ibra composite 1 and 2 profile	saprolite	70572	1085	120	3421	3000	0	10.5	33.5	0.3	43.9	0.2	10.5	0.0	0.2	9.2
	oxide	239609	1869	600	16421	9000	1000	63.3	42.8	0.6	76.7	0.7	57.3	1.5	3.2	36.6
	silcrete	56706	3235	150	6158	3000	100	7.5	15.0	0.4	30.0	0.3	58.0	0.6	0.5	8.9
	clay bed	45603	171	3597	2053	1000	100	10.0	13.2	14.2	57.4	0.3	19.4	27.2	20.2	2.9
East Ibra profile 3	protolith	59172	1264	600	2737	2000	100	30.0	28.8	0.1	22.2	<0.1	8.0	<0.5	0.1	16.6
	oxide /clay	233455	1373	600	18473	7000	100	60.7	46.3	0.4	42.9	0.8	29.1	1.6	1.8	33.9
	silcrete	33433	360	2398	1368	1000	100	12.0	26.9	8.3	20.0	0.5	37.6	16.9	0.9	2.7
	clay	73265	1469	2998	2737	3000	100	24.5	44.5	6.6	80.5	0.9	170.0	14.7	9.8	8.7
Al-Russayl profile 1	oxide	270732	450	1199	51315	7000	100	59.3	130.6	0.6	124.0	1.7	5.6	7.0	4.1	42.5
	silcrete	48540	82	3597	5474	100	100	9.0	13.8	0.8	46.7	1.2	8.6	1.4	2.7	1.9
	ferricrete	508066	227	1199	26000	2000	100	49.0	47.7	0.4	459.0	1.8	22.6	1.2	5.1	10.2
Al-Russayl composite 2 & 3 profile	protolith	57423	765	1269	2737	2000	100	6.0	18.6	0.1	43.9	<0.1	7.9	<0.5	0.2	6.0
	clay	374335	6163	1199	26684	13000	1000	28.7	95.8	2.0	61.3	1.5	34.9	3.6	5.3	35.9
	saprolite	42875	676	60	2053	2000	100	10.0	17.6	0.1	113.0	<0.1	13.4	<0.5	0.1	3.9
	mixture/ (Fe/clay)	101068	2010	600	13000	3000	100	27.5	31.6	1.4	89.1	0.8	68.1	2.8	7.0	9.9
Tiwi profile 1	protolith	49729	673	60	2737	2000	100	9.0	12.2	-	14.4	< 0.1	8.0	-	0.1	6.2
	saprolite	55482	754	60	2737	2000	100	11.3	17.2	0.2	36.0	0.2	10.4	< 0.5	0.1	6.1
	clay bed	375594	1908	1799	19158	3000	1000	301.0	44.7	3.5	155.0	5.9	31.2	2.1	24.6	33.4
	oxide	432418	584	1799	26684	4000	100	81.7	37.1	0.2	90.4	2.6	16.7	0.9	3.3	49.0
Tiwi profile 2	saprolite	65816	853	90	2737	2000	100	9.8	18.1	0.3	34.2	0.1	6.9	<0.5	0.1	6.1
	oxide/ ferricrete	249417	1043	600	13000	6000	100	56.8	57.0	0.5	54.8	1.5	13.8	2.7	0.9	37.5

c. Mass balance

To determine the relative enrichment or depletion of elements relative to the fresh parent rock within the weathering profile during lateritization, we calculated a mass balance. The mass balance model used, according to [15, 20-22] was as follows:

$$\% \text{ change} = [(Xa/Ia)/(Xp/Ip)-1] *100 \quad (1)$$

where X_a and X_p are the concentrations of elements in the weathered samples and in the parent rock, respectively. I_a and I_p are the concentrations of the immobile element in the weathered samples and in the parent rock, respectively.

In this calculation, the average density of rocks was taken in consideration. For parent rock, the measured average density is about 2.6 g per cubic cm, while for the laterite an average density of about 2.5 g per cubic cm was measured.

Elements such as Th, Zr and Ti have been considered as immobile elements during weathering in previous studies [1, 21, 23-25]. In this study, the selection of immobile elements was established after a statistical investigation. In fact, statistical treatment of data revealed similar variations of concentrations of Ti and Th and Zr. However, since

Ti has been considered an immobile element during weathering of mafic rocks, for the mass balance calculation during this study the normalization of Ni, Co, V, Zn, Pb, Sr, Sc, and Cr was established relative to Ti.

Quantification of loss and gain of elements during lateritization was determined for each zone of each profile relative to the parent rock. The results are shown in Table 2 as an average of the results for different depths from the same zone.

The mass balance calculation for Ibra revealed a depletion of most of the elements in all zones. Only V and Pb are enriched in the oxide and clay zones relative to the other elements (Figure 3). The elements Sc and Cr are well correlated with Fe (r = 0.7 and 0.6 respectively), while Ni, Zn, Co and Sr tend to be associated with Mn rather than with Fe.

The mass balance calculation for East Ibra composite profile 1 and 2 showed an enrichment of elements in the saprolite, oxide (upper and lower zones), and silcrete zones, except for Zn which is depleted in the upper oxide zone while V and Sc are depleted in the silcrete zone. Element-element correlations indicate that Cr, Co, Ni and Zn are more strongly associated with Fe oxide than with Mn oxide. Correlation coefficients with Fe are about 0.96, 0.97, 0.9 and 0.8 for Cr, Co, Ni and Zn respectively.

For East Ibra profile 3, only upper and lower oxide zones are characterized by an enrichment in elements. The clay bed is depleted in Ni, Co, V, Sr, Zn, Sc and Cr and enriched in Ba and Pb, while the silcrete layer is depleted in all elements. In this profile, most elements are more concentreted with Fe than with Mn as the case of East Ibra composite 1 and 2 profile. Al and Ni substitution in natural iron oxides (goethite, hematite and maghemite) from laterites has been previously studied [26, 27]. Ni has been found more frequently with goethite but not with Mn oxides. In contrast, [28] reported that Ni might be associated with Mn oxides more than with Fe oxides in a Philippine laterite.

The lateral distribution of elements within every section of the Al-Russayl profile showed that all elements have been mobilized during lateritization, which has resulted in a zone of enrichment in the oxide in the Al-Russayl profile 1 and a depletion of elements in the silcrete zone and a depletion of Ni, Co and Ba in parallel to an enrichment in the other elements in the ferricrete zone of the same profile relative to the fresh protolith. For Al-Russayl composite 2 and 3 profile, the weathering has induced an enrichment of elements in all investigated zones, except Ba which is depleted in the clay zone. Investigation of correlations between elements of Al-Russayl profiles indicates that Ni is well correlated with Mn, while Cr and Zn are more associated with Fe than Mn oxides, and Co, Sr and Sc levels do not indicate any correlation with either Fe or Mn.

Table 2. Mass balance data of the different laterite profiles.

Profile	Element/ Zone	Ni	Co	V	Zn	Sr	Ba	Pb	Sc	Cr
Ibra	saprolite	-100	-100	-3	-97	-86	-98	-98	-92	-100
	oxide	-81	-63	360	-95	-74	-93	183	-69	-18
	Clay	-77	-48	182	-94	-70	-89	656	-72	14
E. Ibra composite 1 & 2 profile	saprolite	563	355	-3	381	767	402	395	110	386
	lower oxide	769	392	29	270	1121	891	829	67	768
	upper oxide	199	178	20	-25	49	292	1412	62	246
	silicrite	269	254	-38	25	228	1632	772	-98	501
E. Ibra profile #3	lower oxide	809	506	-39	266	549	382	163	55	424
	upper oxide	174	163	28	-10	-3	153	754	55	397
	clay bed	-77	-56	-91	-82	-57	157	682	-92	-90
	silcrete	-88	-86	-94	-87	-88	-35	-11	-97	-94
Al Russayl profile #1	oxide	181	-20	692	463	126	1544	1544	468	1403
	silcrete	-100	-73	-60	-80	-72	-97	261	-92	-47
	ferricrete	-20	-20	555	106	738	-78	1945	36	662
Al-Russayl composite 2 & 3 profile	saprolite	1502	1502	2570	1416	4024	121	701	941	1102
	clay	421	702	284	313	12	-74	2025	380	682
	mixture/(Fe/clay)	140	60	634	172	225	3	5508	1719	661
Tiwi profile #1	saprolite	-24	-24	-5	7	89	52	-24	-25	-24
	oxide laterite	-96	-75	-15	-91	-73	-96	522	-86	-82
	clay bed	-95	-97	-77	-92	-84	-92	-17	-80	-75
Tiwi profile #2	saprolite	-49	-49	-45	-25	20	-58	-49	-50	-49
	oxide/ferricrete	-77	-92	-52	-65	-71	-97	-32	-54	-64

For the Tiwi area, a mass balance for the two profiles (1 and 2) was calculated. Profile 1 is about 40 m thick from topsoil to bedrock, and represents the complete profile, while profile 2 is about 30 m thick. The mass balance calculation indicates that all investigated zones in Tiwi profile 1 are characterized by a depletion of elements, with the exceptions of Pb which is enriched in the oxide zone, and of Sr and Ba which were found enriched in the saprolite zone. In Tiwi profile 2, all elements are depleted relative to the parent rock, except for Sr which is slightly enriched in the saprolite zone. Elements such as Cr and Zn are more concentrated with Fe than with Mn, while Co and Ni seem be carried by both Fe and Mn oxides [12]. The mass balance calculation using equation (1) in this study is coherent with values calculated using the model reported by Braun [26] for calculation of the mass balance of elements in a lateritic terrain. In this previous study, the volume change in each zone of the soil, due to weathering, is considered in the calculation model. The calculation of the volume change in the present study indicated a decrease in the volume of the Ibra profile due to collapse during weathering, while in the East Ibra composite 1 and 2 profile, there was an expansion of the soil during weathering. Such differences may reflect different paloclimatic conditions.

5. Discussion

The rate of accumulation of elements in soils depends on the susceptibility and resistance of rocks to weathering, the leaching process of elements, and their adsorption or fixation on clay and oxide phases. The mobility and accumulation of trace elements in the soil during weathering depends on their distribution between different mineral phases.

The different zones of the investigated laterite profiles (Ibra, East Ibra, Tiwi and Al-Russayl) vary in mineral composition and in the thickness of each zone. The zones of Ibra profile are thicker than the zones in the other profiles, which may reflect an important weathering process and longer time of lateritization compared to the other profiles. Moreover, Ibra profile is characterized by a development of different zones during weathering, such as oxide, saprolite and clay zones, unlike other profiles where either the saprolite zone (as in the case of East Ibra profile 3) or the clay zone (as in Tiwi profile 2 and Al-Russayl profile 1) are missing. In terms of chemical composition, most of the elements investigated during this study do not exhibit the same fluctuations and behavior in the different zones of each profile. For example, in the East Ibra sections, enrichment of elements occurred in the saprolite, silcrete and oxide zones while in Al-Russayl composite 2 and 3 profile, the enrichment which was calculated for elements occurred in the saprolite zone and exceeded that calculated for the same zone in the other profiles.

a. Mobilization of elements during laterization

Mass balance calculations relative to the fresh parent rock indicated that the mobilization of elements in each profile is dissimilar, and may indicate different weathering histories and different degrees of serpentinization. The laterite soil in the present study was developed on ophiolite rocks with slight differences between parent rocks in each section. The differences between sections in terms of geochemistry and mineral content may reflect differences in weathering conditions, including topography and drainage.

The enrichment in heavy metals in soil zones is often inherited from the parent rock. Their vertical distribution is controlled by their mobility during chemical weathering, adsorption by clay particles, the concentration of organic matter in the soil, and by their precipitation or their complexation with different ions.

The variability in mobilization of elements during weathering can be expressed as a ratio between elements. The investigated ratios consist of Ni/Co, Ni/Cr and Ni/Zn. The Ni/Zn ratio increases in the following order: clay zone > oxide zone > saprolite for Ibra profile, while the Ni/Co ratio is similar in oxide and clay zones. In the oxide and saprolite zones of this profile, the Ni/Zn and Ni/Co ratios are higher than in the parent rock, unlike the Ni/Cr ratio, which is lower. In the clay zone, both the Ni/Cr and Ni/Co ratios are lower than in the parent rock, while the Ni/Zn ratio is higher. Investigation of these different ratios in different zones of Ibra profile indicates the following order of mobility of elements: Ni>Co>Zn.

In East Ibra composite 1 and 2 profile, the Ni/Zn ratio in each zone is higher than that of the parent rock, which reflects the higher mobility of Ni and Cr relative to Zn and Co. The Ni/Cr and Ni/Co ratios, on the other hand, are lower in the oxide and clay zones than in the parent rock.

In East Ibra profile 3, the Ni/Zn ratio in the oxide zone is higher than in the parent rock, while the clay zone has a similar Ni/Zn ratio to the parent rock. The Ni/Cr ratio in the oxide zone is lower than in the parent rock, but the opposite is the case in the clay zone while the Ni/Co ratios in both oxide and clay zones exceed that of the parent rock. Comparison between the different zones indicates that the highest Ni/Zn and Ni/Co ratios characterize the oxide zone, and the highest Ni/Cr ratio characterizes the clay zone.

For Al-Russayl profile 1, the Ni/Zn and Ni/Cr ratios in the oxide zone are lower than in the parent rock, unlike the Ni/Co ratio. For Al-Russayl composite 2 and 3 profile, the Ni/Zn ratio in the clay zone is higher than in the parent rock , opposite to the Ni/Co ratio for the same zone. In the saprolite zone, Ni/Zn, Ni/Cr and Ni/Co ratios remain similar to those of the parent rock.

For Tiwi section, the Ni/Zn ratio in the saprolite, clay and oxide zones is lower than in the parent rock. The Ni/Cr ratio in the clay and oxide zones is lower than in the parent rock, while the Ni/Co ratio in the oxide zone exceeds the Ni/Co ratio of the parent rock.

Ni, Zn, Cr, and Co are usually incorporated in the lattice of silicate or oxide minerals. Higher Ni/Zn and Ni/Cr ratios in the clay zones of Ibra, Al-Russayl composite 2 and 3 profile and East Ibra 3 compared to the other zones, and additionally, a higher Ni/Co ratio in the Fe- clay zone of Al-Russayl composite 2 and 3 profile, reflect the higher exchange capacity for Ni in the clay zone. The association of Ni with Fe-Mn oxides results in higher Ni/Zn, Ni/Co and Ni/Cr ratios in the oxide zone, as in East Ibra profile 3.

A saprolite zone (usually called the C zone or partially altered bedrock zone) is between the subjacent fresh or non-weathered parent rock zone and the superjacent clay/iron oxide zone (which is also called the B zone or zone of leaching). The saprolite zone then contains some metals that are produced from *in situ* weathering of minerals of the parent rock, and some that may have come from the overlying zones. Therefore, the apparent increase of the Ni/Cr ratio in the saprolite zone of Ibra, East Ibra and Al-Russayl profiles compared to their parent rocks reflects the selective thermodynamic binding of the metals, or the stability constants of the metals with available ligands or chelates in the weathering zones. The selections are therefore influenced by (i) charge, (ii) ion size, (iii) ligand donor atoms, (iv) preferential coordination geometry or stereochemical control, (v) oxidation states, and for the transitional metals, (vi) spin-pairing stabilization [29-32].

In normal aqueous media, association of Co to Zn can be found in oxidation states of 2+. While Ni, Co, Zn and Cr can co-ordinate with water for hydrolysis reactions, they are also able to form bonds with S-donor ligands. Smaller high charged ions are more strongly hydrated than larger low charged ions. Replacement of coordinated water molecules around a smaller cation by organic ligands requires higher energy. Therefore, a Ni/Zn increase in the saprolite zone may be explained in terms of the relatively higher mobility of Ni influenced by the hydration effect, as well as by the ligand co-ordination effect. An increase in the Ni/Co ratio may be the result of a redox reaction effect, possibly in the upper organic-rich zone, besides the latter having a preference for O-donor ligands.

b. Redox conditions: Ce occurrence in the soil

As mobilization of Ce during weathering is sensitive to redox conditions, an investigation of the correlation of Ce with elements such as Mn, Ni, Co, Fe and Cr indicated that Ce exhibits three oxidation states, +II, +III and +IV. The first of these is not common. Among these states, Ce(III) is soluble in a reduced environment, but the oxidized state of Ce (Ce IV) is insoluble [6]. In Ibra profile only Co and Zn are well correlated with Ce, unlike Ni, Fe, Mn and Co. In East Ibra composite 1 and 2 profile, weak correlations were calculated between Ce and Cr, Mn, Fe, Co and Ni. In East Ibra 3 profile the mobilization of Co, Cr and Ni, which are well correlated with Ce, seems to be affected by fluctuations of redox conditions in this profile. The increase of Ce in this soil, due to the oxidation of Ce(III) to the less soluble Ce (IV), correlates to a leaching of Cr, Fe and Ni from the soil.

In Al-Russayl profile 1 good correlations were calculated between Ce and Mn ($r = 0.93$), Co ($r = 0.86$), Ni ($r = 0.9$), Zn ($r = 0.98$) but not with Fe, while in Al-Russayl composite 2 and 3 profile, Ce is well correlated with Ni, Mn and Fe, but not with Co and Cr. In Tiwi profile 1 and Tiwi profile 2, Cr, Ni and Zn seem to be affected by redox conditions of the soil since they exhibit good correlations with Ce.

c. Sc-Fe interaction in the soil

Although the soil chemistry for scandium (Sc) is similar to that for Fe and substitutes Fe^{3+} in primary minerals, Sc is not affected by redox reactions. According to Brown [33] in lateritic soils the Fe-accumulation, lacking any redox influences, can be estimated from the Sc/Fe ratio. This Fe accumulation is highlighted by the deviation of samples from the Sc-Fe linear relationship.

The Sc/Fe ratio in different zones from different sections investigated during this study is about $0.09.10^{-3}$ to $0.16.10^{-3}$. The oxide zones of Tiwi 1 and Ibra profiles and the clay zone of Tiwi profile 1 and Al-Russayl composite 2 and 3 profile are characterized by lower Sc/Fe ratios because of significant accumulation of Fe as compared to that of Sc (Figure 4). This enrichment of Fe independently of redox conditions might reflect adsorption of Fe on clay minerals, and/or a deposition of amorphous Fe during the laterization processes.

All zones of Al-Russayl composite 2 and 3 profile are characterized by similar ratios to that of the parent rock, which indicates a homogeneity in the distribution of these two elements during the laterization processes.

In Ibra profile, the Sc/Fe ratio in all zones is similar to that of the parent rock except in the serpentinized zone, where a high concentration of Fe and low concentration of Sc generate a lower Sc/Fe ratio than in the parent rock. In all zones of East Ibra composite 1 and 2 profile, the Sc/Fe ratio is lower than in the parent rock because of the significant concentration of Fe in the saprolite and the oxide zones, and because of an important depletion of Sc in the silcrete and the clay zones. Similar to the East Ibra composite 1 and 2 profile, all zones of East Ibra profile 3 are characterized by lower Sc/Fe compared to the parent rock.

In Tiwi profile 1, the clay zone is characterized by an important accumulation of Fe which generates a Sc/Fe ratio lower than that of the parent rock. The other zones of Tiwi profile 1 have a Sc/Fe ratio similar to that of the parent rock. The oxide zone of Tiwi profile 2 is characterized by an important deposition of Sc compared to the parent rock, which induces a Sc/Fe ratio higher than that of the parent rock.

d. Rate of weathering and accumulation rate of Ni

An estimation of the duration of lateritization by Lucas [34] indicated that about 17 to 34 million years (my) are needed to form a profile. The average thickness of the Ibra profile of the present study is about 60 m (20 m for the layered gabbro zone, 20 m for the saprolite zone, 5 m for the oxide zone, 15 m for the clay zone). Such a thickness corresponds to a rate of downward advance of the weathering front of 3 m per million years (my) if an average duration of 20 my is considered. Such a rate might be overestimated or underestimated if all weathering conditions are taken into consideration. However, the leaching and distribution of elements may be accelerated for young profiles and under humid climate conditions [35]. Based on a density of 2.5 g/cubic cm, we estimated that about 4000 g of Ni may be extracted per 1my from 1 square meter of the layered gabbro zone developed in Ibra profile and about 6000 g per 1my from 1 square meter of the saprolite zone and 2500 g per 1my from 1 square meter of the oxide zone and about 12000 g per 1 my from 1 square meter of the clay zone.

Similar estimations calculated for East Ibra profiles showed that more Ni can be extracted from the oxide zone of East Ibra composite 1 and 2 profile than from the other zones of either the same profile or the East Ibra profile 3. In contrast, the clay zone of East Ibra profile 3 accumulated more Ni than the clay zone in the East Ibra composite 1 and 2 profile.

e. Dynamic of Th and U

Thorium occurs in diverse rock types in association with U and rare earth elements. Thorium is very insoluble during weathering compared to U.

The U–Th couple is useful in constraining paleo-redox conditions because ^{232}Th, ^{235}U, and ^{238}U are long-lived radionuclides, which decay to different Pb isotopes. Th/U ratios may represent different stages of oxidation and leaching. Th/U ratios may be used to estimate paleo-redox conditions at the time of deposition [36].

In oxidized environments, sediments may contain less U, and show high Th/U ratios above the average upper continental crust ratio of 3.8 [37]. In sediments deposited in a reduced environment, the Th/U ratio is low [38-40]. The Th/U ratio is controlled by the weathering-erosion-diagenesis cycle [41].

Due to large differences in Th and U concentrations through different profiles, discussion of the Th/U ratio will be based on data of individual profiles and not composed ones, as was done for mass balance calculations (Table 3).

In Ibra profile, the Th/U ratio ranges from 0.5 to 6.0 for the clay zone. For East Ibra 1 profile, the average ratio is about 2.25. The other investigated zones are characterized by lower Th and U concentrations, of less than the detection limit. For East Ibra composite 2 and 3 profile, an average Th/U ratio of about 4.4 was calculated for the upper oxide zone.

Table 3. U/Th ratio of the different laterite profiles.

Ibra Profile			
zone	Th (ppm)	U (ppm)	Th/U
clay laterite	0.6	0.1	6.0
	1.4	0.8	1.8
	0.5	0.9	0.6
oxide laterite	2.7	3.5	0.8
	1.9	0.8	2.4
	0.4	0.4	1.0
	0.6	0.6	1.0
	0.5	0.2	2.5
	0.5	0.3	1.7
saprolite	< 0.1	< 0.1	-
	< 0.1	< 0.1	-
	0.1	< 0.1	-
	0.2	< 0.1	-
protolith	< 0.1	0.2	-
	< 0.1	< 0.1	-
	< 0.1	< 0.1	-
	0.2	< 0.1	-
	0.1	< 0.1	-

Table 3 (cont.). U/Th ratio of the different laterite profiles.

E Ibra profile 1				E Ibra composite 2 and 3 Profile			
zone	Th (ppm)	U (ppm)	Th/U	zone	Th (ppm)	U (ppm)	Th/U
clay bed	1.8	0.8	2.25	U oxide laterite	0.77	0.18	4.4
U oxide laterite	0.5	< 0.1	-	L oxide laterite	<0.1	< 0.1	-
L oxide laterite	0.4	< 0.1	-	saprolite	< 0.1	< 0.1	-
	< 0.1	< 0.1	-	protolith	< 0.1	< 0.1	-
saprolite	0.1	< 0.1	-				
	< 0.1	< 0.1	-				

Al-Russayl profile 1				Al-Russayl composite 2 and 3 profile			
zone	Th (ppm)	U (ppm)	Th/U	zone	Th (ppm)	U (ppm)	Th/U
ferricrite	1.2	1.5	0.8	clay bed	1.4	0.5	2.8
oxide	1.3	0.5	2.6	oxide (limonite)	0.9	0.6	1.6
pockets green clay	2.2	2.5	0.9	clay laterite	1.6	0.3	5.4
	0.6	0.7	0.9	saprolite	0.1	0.2	0.5
	1.7	0.7	2.4	protolith	< 0.1	< 0.1	
ferricrite	1.4	0.1	14.0				

Tiwi profile 1			
zone	Th (ppm)	U (ppm)	Th/U
clay bed	3.6	11.7	0.3
oxide	4.8	7.0	0.7
	1.4	4.1	0.3
	1.6	4.8	0.3
	0.5	3.9	0.1
	0.4	4.1	0.1
	0.5	3.7	0.1
	0.3	3.8	0.1
saprolite	< 0.1	< 0.1	-
	< 0.1	< 0.1	-
	< 0.1	< 0.1	-
	0.2	0.3	0.7
protolith	< 0.1	< 0.1	-
	< 0.1	< 0.1	-

Tiwi profile 2			
zone	Th (ppm)	U (ppm)	Th/U
ferricrite	0.4	2.8	0.1
oxide	< 0.1	1.3	-
ferricrite	< 0.1	< 0.1	-
saprolite	< 0.1	< 0.1	-
	< 0.1	< 0.1	-
	0.1	< 0.1	-
	< 0.1	< 0.1	-

The Th/U ratio in Al-Russayl profile 1 is about 0.9 to 14. The highest values were calculated for the ferricrete zone. In Al-Russayl composite 2 and 3 profile, the Th/U ratio is lower than that of Al-Russayl profile 1, and ranges from 0.5 to 5.4, with the highest value for the clay zone. For both Tiwi profile 1 and Tiwi profile 2, the Th/U ratio is < 1.

Large fluctuations of the Th/U ratio may be attributed to either the source or redox conditions in the profile. Fluctuation of Th concentrations may reflect different sources through the profile, while different concentrations of U reflect fluctuations in redox potential. The high Th/U ratio (above that of continental crust) in the Al-Russayl profile

and all East Ibra profiles may indicate an oxidizing environment, while the low Th/U ratio (<1) in the Tiwi profiles is indicative of a reducing environment.

6. Conclusion

Investigation of laterite soils in Oman which have developed on mafic/ultramafic rocks revealed differences in the thickness of the same zones (e.g. saprolite, oxide etc…) formed in different profiles. Moreover these different profiles are characterized by a heterogeneous distribution of elements. Such differences imply different conditions of weathering (differences in the local conditions of climate and topography). To estimate the gain and loss of elements through each profile, a mass balance was calculated, which showed that all elements have been mobilized and transferred downwards along the profile.

The mass balance calculation for Ibra profile relative to the parent rock revealed that most elements have been depleted in the saprolite, oxide, clay and ferricrete zones. In East Ibra composite 1 and 2 profile, the mass balance calculation showed that all elements were enriched in the saprolite, oxide and silcrete layers and depleted in the clay zone, relative to the parent rock. In East Ibra profile 3, only the oxide zone was enriched in all elements during weathering. For Al-Russayl profile 1, all elements were enriched in the oxide zone and depleted in the silcrete zone, while in Al-Russayl composite 2 and 3 profile, an enrichment in all elements was calculated in all investigated zones.

For both Tiwi profiles (1 and 2), all investigated zones are characterized by a depletion in elements. Redox conditions during weathering were investigated using the correlation of elements with Ce on the one hand, and Th/U and Sc/Fe ratios on the other hand.

Investigation of Sc/Fe ratios in different zones indicated low values for Tiwi 1 and Ibra profiles and Al-Russayl composite 2 and 3 profile due to an important accumulation of Fe independently of redox conditions. Large fluctuations characterize the Th/U ratios in all profiles, and indicate that the weathering in Al-Russayl and East Ibra composite 1 and 2 profiles and East Ibra profile 3 might have been characterized by a more oxidizing environment than was the weathering in the Tiwi profiles.

7. Acknowledgements

The authors would like to sincerely thank Saif Al Maamari for XRD analyses and all those technicians who have contributed through preparation of samples. Research grant (#IG/SCI/ETHS/07/03) from Sultan Qaboos University is gratefully acknowledged.

References

1. Al-Khirbash, S., Semhi, K, Richard, L. and Nasir, S. Rare earth element mobility during laterization of mafic rocks of the Oman ophiolite. *Arab J Geosci.,* 2013b. *DOI 10.1007/s12517-013-1189-6.*
2. Zeissink, H.E. Trace elements behaviour in two nickeliferous laterite profiles. *Chem.Geol.,* 1971, **7**, 25-36.
3. Evans, A.M. Ore Geology and Industrial Minerals — An Introduction. Blackwell, London, 1993, p389.
4. Nayak, B.K., Das, S.K., Rajeev, S.K., Muralidhar, J., and Sahoo, R.K. Four-dimensional trend surface analysis and its implications on the distribution of Ni, Co, Fe_2O_3, Cr_2O_3, SiO_2 and Al_2O_3 in the nickeliferous laterite overburden of South Kaliapani chromite deposit, Sukinda ultramafic belt, Orissa, India. *J. Min. Petr. Econ. Geol*., 1998, **93**, 195-206.
5. Hill, I.G., Worden, R.H., and Meighan, I.G. Geochemical evolution of a palaeolaterite: the Interbasaltic Formation, Northern Ireland. *Chemical Geol.*, 2000a, **166 (1)**, 65-84.
6. Jin-Long, MA., Gang-Jian Wei, Yi-Gang Xu, Wen-Guo Long, and Wei-Dong Sun. Mobilization and re-distribution of major and trace elements during extreme weathering of basalt in Hainan Island, South China. *Geochimica et Cosmochimica Acta*, 2007, **71**, 3223-3237.
7. Elias, M., Donaldson, M.J., and Giorgetta, N. Mineralogy and geochemistry of lateritic nickel cobalt deposits near Kalgoorlie, Western Australia, *Econ. Geol.*, 1981, **76**, 1775-1783.
8. Elias, M. Nickel laterite deposits – Geological overview, resources and exploitation. In Giant ore Deposits: Characteristics, Genesis and Exploration (Eds. David, R.C. and June, P.) *Codes Special Publication* 2002, **4**, 205–220.
9. Gleeson, S.A., Butt, C.M.R., and Andelias, M. Nickel laterites: a review, *SEG Newsletter Soc. Econ. Geosci.*, 2003, **54**, 9–16.
10. Gleeson, S.A., Herrington, R.J., Durango, J., Velazquez, C.A., and Koll, G. The mineralogy and geochemistry of de Cerro Matoso S. Ni laterite deposit, Montelíbano, Colombia. *Econ Geol.,* 2004, **99**, 1197–1213.
11. Sagapoa, C.V., Imai, A., Ogata, T., Yonezu, K., and Watanabe, K. Laterization Process of Ultramafic Rocks in Siruka, Solomon Islands. *J. SE Asian Appl. Geol.,* 2011, **3(2)**, 76-92.
12. Al-Khirbash, S. Genesis and Mineralogical Classification of Ni-laterites, Oman Mountains. *Ore Geol. Rev.,* 2015, **65**, 199–212.
13. Goodenough, K.M., Styles, M.T., Schofield, D., Thomass, R.J., Crowley, Q.C., Lilly, R.M., McKervey, J., Stephenson, D., and Carney, J.N. Architecture of the Oman–UAE Ophiolite: Evidence for a multi-phase magmatic

history. In Lithosphere Dynamics and Sedimentary Basins: The Arabian Plate and Analogues Frontiers in Earth Sciences (Eds. Al Hosani, K., Roure, R., Ellison, R., and Stephen, L.). 2013, 23-42. doi 10.1007/978-3642-30609-9.

14. Glennie, K.W., Bœuf, M.G.A., Hughes, C.W., Moody-Stuart, M., Pilaar, W.F.H., and Reinhardt, B.M. Late Cretaceous nappes in the Oman Mountains and their geologic significance. *Am Assoc of Petroleum Geologists Bull*., 1973, **57**, 5-27
15. Colman, S.M. Chemical weathering of basalts and andesites: evidence from weathering rinds. *U.S. Geol. Surv. Prof. Pap*., 1982, **1246**, 1-51.
16. Al-Khirbash, S., Nasir, S., Al-Harthy, A., Richard, L., Al-Sayigh, A., Darkel, A., and Semhi, K. Geology and Ni-Co Mineralization of Laterites of the Oman Mountains, *7th International Symposium on the Eastern Mediterranean Geology, 18-22 October, 2010, Cukurova University, Adana – Turkey*
17. Al-Khirbash, S., Richard, L., Nasir, S., Al-Sayigh, A., and Semhi, K. Geology and economic potentiality of Ni-laterites in the Oman Mountains, *10th meeting of the Saudi Society for Geoscience, Dhahran, April 15-17, 2013a.*
18. Rollinson, H.R., Searle, M. P., Abbasi, I.A., Al-Lazki, A., and Al Kindi, M. Tectonic evolution of the Oman Mountains: an introduction. In *Tectonic Evolution of the Oman Mountains.* (Eds. Rollinson, H.R., Searle, M. P., Abbasi, I.A., Al-Lazki, A., and Al Kindi, M.), Geological Society of London Special Publication, London. 2014, **392**, 1–7. http://dx.doi.org/10.1144/SP392.1.
19. Abbasi, I. A., Salad Hersi, O. and Al-Harthy, A. Late Cretaceous conglomerates of the Qahlah Formation, north Oman. In *Tectonic Evolution of the Oman Mountains.* (Eds. Rollinson, H.R., Searle, M. P., Abbasi, I.A., Al-Lazki, A. and Al Kindi, M.), Geological Society of London Special Publication, London. 2014, **392**, 325–341. http://dx.doi.org/10.1144/SP392.17.
20. Chesworth, W., Dejou, J., and Larroque, P. The Weathering of basalt and relative mobilities of the major elements at Belbex, France. *Geochimica et Cosmochimica Acta*, 1981, **45**, 1235–1243.
21. Middelburg, J.J., Weijden Van Der, C.H., and Woittiez, J.R.W. Chemical processes affecting the mobility of major, minor and trace elements during weathering of granitic rocks. *Chem. Geol*., 1988, **68**, 253-273.
22. Ndjigui, P.D., Bilong, P., Bitom, D., and Dia, A. Mobilization and redistribution of major and trace elements in two weathering profiles developed on serpentinites in the Lomié ultramafic complex, South-East Cameroon. *J. African Earth Sciences*, 2008, **50 (5)**, 305-328.
23. Nesbitt, H.W. Mobility and fractionation of rare earth elements during weathering of a granodiorite, *Nature*, 1979, **279**, 206 - 210.
24. Gouveia, M.A., Prudencio, M.I., Figueiredo, M.O., Pereira, L.C.J., Waerenborgh, J.C., Morgado, I., Pena, T., and Lopes, A. Behaviour of REE and other trace and major elements during weathering of granitic rocks, Evora, Portugal. In Geochemistry of the Earth Surface. (L.R. Kump, L.R., Guest Editor), *Chem. Geol.*, 1993, **107**, 293-296.
25. Hill, I.G., Worden, R.H., and Meighan, I.G. Yttrium: the immobility-mobility transition during basaltic weathering. *Geology*, 2000b, **28 (10)**, 923–926.
26. Braun, J.J., Marechal, J.C., Riotte, J., Bbeglin, J.L., Bedimo, J.P., Ndam Ngoupayou, J.R., Brunot Nyeck, Robain, H., Sekhar, M., Audry, S. and Viers, J. Elemental weathering fluxes and saprolite production rate in a Central African lateritic terrain (Nsimi, South Cameroon). *Geochimica et Cosmochimica Acta*, 2012, **99**, 243–270.
27. Trolard, F., Bourrie, G., Jeanroy, E., Herbillon, A.J., and Martin, H. Trace metals in natural iron oxides from laterites: A study using selective kinetic extraction. *Geochimica et Cosmochimica Acta*, 1995, **59(7)**, 1285-1297.
28. Fan, R., and Gerson, A.R. Nickel geochemistry of a Philippine laterite examined by bulk and microprobe synchrotron analyses. *Geochimica et Cosmochimica Acta*, 2011, **75**, 6400–6415.
29. Stahl, R.S. and James, B.R. Zinc sorption by B horizon soils as a function of pH. *Soil Sci. Soc. Am. J.*, 1991, **55**, 1592–1597.
30. Vulav, V. and Seaman, J.C. Mobilization of Lead from Highly Weathered Porous Material by Extracting Agents. *Environ. Sci. Technology*, 2000, **34**, 4828-4834.
31. Covelo, E.F., Andrade, M.L., and Vega, F.A. Heavy metal adsorption by humic umbrisols: selectivity sequences and competitive sorption kinetics. *J. Colloid Interface Sci.*, 2004, **280**, 1–8.
32. Tansupoa, P., Budzikiewiczb, H., Chanthaia, S. and Ruangviriyachai, C. Effect of pH on the mobilization of copper and iron by pyoverdin I in artificially contaminated soils**.** *Science Asia*, 2008, **34**, 287-292.
33. Brown D.J., Helmke P. A., and Clayton M. K. Robust geochemical indicies for redox and weathering on a granitic laterite landscape in central Uganda. *Geochimica et Cosmochimica Acta*, 2003, **67**, 2711–2723.
34. Lucas, Y. Systèmes pédologiques en Amazonie brésilienne: equilibres, déséquilibres et transformations, 1989, *Thèse de Doctorat, Université de Poitiers*.
35. Giral-Kacmarc k , S., Savin, S.M., Girard, J.P., Lucas, Y., and Abel, L. Oxygen isotope geochemistry of kaolinite in laterite-forming processes, Manaus, Amazonas, Brazil. *Geochimica et Cosmochimica Acta*, **62(11)**, 1865-1879.
36. Doveton, J.D. Lithofacies and geochemical facies profiles from nuclear wireline logs: new subsurface templates for sedimentary modelling. In Sedimentary modellingcomputer simulations and methods for improved parameter definition (Eds. Franseen, E.K., Watney, W.L., Kendall, C.J. and Ross, W.), *Kansas Geological Society Bulletin* 1991, **233**, 101-110.

37. Taylor, S.R. and Mclennan, S.M. The Continental Crust: Its Composition and Evolution. Blackwell Scientific, Oxford, 1985, p312.
38. McLennan, S.M. and Taylor, S.R. Th and U in sedimentary rocks: crustal evolution and sedimentary cycling. *Nature*, 1980, **285**, 621-624.
39. Hemming, S.R. and McLennan, S.M. Pb isotope compositions of modern deepsea turbidites. *Earth and Planetary Science Letters* 2001, **184**, 489-503.
40. Krogstad, E., M Fedo, C., and Eriksson, K.A. Provenance ages and alteration histories of shales from the Middle Archean Buhwa greenstone belt, Zimbabwe: Nd and Pb isotopic evidence. *Geochimica et Cosmochimica Acta*, 2004, **68**, 319-332.
41. Condie, K.C. Chemical composition and evolution of the upper continental crust: contrasting results from surface samples and shales. *Chem. Geol.*, 1993, **104**, 1-37.

Received 25 December 2014
Accepted 11 April 2015